

## Spectral shape of one-photon luminescence from single gold nanorods

Te Wen, Yingbo He, Xue-Lu Liu, Miao-Ling Lin, Yuqing Cheng, Jingyi Zhao, Qihuang Gong, Keyu Xia, Ping-Heng Tan, and Guowei Lu

Citation: *AIP Advances* **7**, 125106 (2017);

View online: <https://doi.org/10.1063/1.5008544>

View Table of Contents: <http://aip.scitation.org/toc/adv/7/12>

Published by the [American Institute of Physics](#)

---

### Articles you may be interested in

[Modeling and analysis of the chip formation and transient cutting force during elliptical vibration cutting process](#)

*AIP Advances* **7**, 125101 (2017); 10.1063/1.5006303

[Stability of the helical configuration of an intrinsically straight semiflexible biopolymer inside a cylindrical cell](#)

*AIP Advances* **7**, 125003 (2017); 10.1063/1.5002145

[Separating grain-boundary and bulk recombination with time-resolved photoluminescence microscopy](#)

*Applied Physics Letters* **111**, 233902 (2017); 10.1063/1.5010931

[Dielectric and energy storage performances of PVDF-based composites with colossal permittivity Nd-doped BaTiO<sub>3</sub> nanoparticles as the filler](#)

*AIP Advances* **7**, 125104 (2017); 10.1063/1.5003292

[Modeling and numerical simulation of anode activity and arc motion in a transverse magnetic field](#)

*AIP Advances* **7**, 125006 (2017); 10.1063/1.5001738

[A first-principles study of gas molecule adsorption on borophene](#)

*AIP Advances* **7**, 125007 (2017); 10.1063/1.5005959

---

# HAVE YOU HEARD?

Employers hiring scientists and engineers trust

**PHYSICS TODAY | JOBS**

[www.physicstoday.org/jobs](http://www.physicstoday.org/jobs)



## Spectral shape of one-photon luminescence from single gold nanorods

Te Wen,<sup>1</sup> Yingbo He,<sup>1</sup> Xue-Lu Liu,<sup>2</sup> Miao-Ling Lin,<sup>2</sup> Yuqing Cheng,<sup>1</sup>  
Jingyi Zhao,<sup>1</sup> Qihuang Gong,<sup>1,3</sup> Keyu Xia,<sup>4</sup> Ping-Heng Tan,<sup>2,a</sup>  
and Guowei Lu<sup>1,3,a</sup>

<sup>1</sup>State Key Laboratory for Mesoscopic Physics & Collaborative Innovation Center of Quantum Matter, Department of Physics, Peking University, Beijing 100871, China

<sup>2</sup>State Key Laboratory of Superlattices and Microstructures, Institute of Semiconductors, Chinese Academy of Sciences, Beijing 100083, China

<sup>3</sup>Collaborative Innovation Center of Extreme Optics, Shanxi University, Taiyuan, Shanxi 030006, China

<sup>4</sup>College of Engineering and Applied Sciences, Nanjing University, Nanjing, Jiangsu 210008, China

(Received 7 October 2017; accepted 28 November 2017; published online 7 December 2017)

Light emission from gold nanoparticles was investigated with ultra-narrow-band notch filters to obtain the complete spectral shape. The anti-Stokes emission band was observed at all excitation wavelengths. The spectral shape of the anti-Stokes emission could be well fitted by a Fermi–Dirac-like line shape, while the spectral profile of the Stokes emission could be fitted by a Lorentzian line shape. The electron distribution and local surface plasmon resonance jointly determined the spectral shape. Additionally, we found that the anti-Stokes emission intensity increased more rapidly compared with that of the Stokes emission as illumination power was increased. This phenomenon can be understood from the temperature dependence of the electron distribution owing to photothermal effects. © 2017 Author(s). All article content, except where otherwise noted, is licensed under a Creative Commons Attribution (CC BY) license (<http://creativecommons.org/licenses/by/4.0/>). <https://doi.org/10.1063/1.5008544>

### INTRODUCTION

Weak luminescence, or photoluminescence (PL), is a well-known phenomenon.<sup>1–3</sup> Photoluminescence was first supposed to arise from interband transitions, and it is enhanced by localized surface plasmon (LSP) resonance. Later, intraband transitions were proposed to explain strong infrared emission.<sup>4,5</sup> The PL spectrum of gold nanoparticles invariably follows the plasmon resonance band of the particle.<sup>6</sup> Such spectral coincidence can be tuned from the visible to the infrared.<sup>7,8</sup> This spectral coincidence has been verified mainly from Stokes emission, whereas anti-Stokes emission has received little attention. Anti-Stokes emission was reported in 1969, and attributed to recombination of thermal smearing of the electron and hole.<sup>1</sup> In recent work, anti-Stokes emission was defined as an up-converted luminescence process.<sup>9</sup> Anti-Stokes emission was found to be enhanced by over three orders of magnitude compared with that of the bulk gold.<sup>10</sup> However, in previous measurements, optical filters with a notch band of tens of meV were applied to block elastic scattering of the excitation. This approach prevents observation of the full-spectral line shape close to the excitation wavelength, and different groups have drawn various conclusions, with discrepancies in those explanations. For instance, Huang et al. introduced a Bose-Einstein-like distribution to fit the emission spectra,<sup>11</sup> resulting in divergence of the fitting spectrum at the excitation wavelength. Conversely, He et al. claimed that the electron occupation followed the Fermi–Dirac distribution and the profile of the anti-Stokes emission could be applied to probe the localized temperature in principle.<sup>10,12</sup> Full spectra might help to elucidate the electron

<sup>a</sup>E-mail: [phtan@semi.ac.cn](mailto:phtan@semi.ac.cn), [guowei.lu@pku.edu.cn](mailto:guowei.lu@pku.edu.cn)

and hole occupation, however, it is necessary to reveal the line shape close to the excitation wavelength.

In this study, we measured the light emission spectra of single gold nanorods (GNRs) using BragGrate™ notch filters with an ultra-narrow bandwidth based on volume Bragg Grating (VBG), hereafter denoted as VBG-based notch filters. This approach enabled us to observe both Stokes and anti-Stokes emission spectra simultaneously with a blocking bandwidth of  $\sim 1$  meV. We confirmed that the Stokes emission spectral shape featured a Lorentzian line shape, while the anti-Stokes emission spectral shape could be fitted well with a Fermi–Dirac-like line shape. A clear anti-Stokes emission band was present at all excitation wavelengths examined. We also found that the anti-Stokes emission intensity increased more rapidly than that of Stokes emission as the temperature was increased.

To measure the spectra of single gold nanorods, dark-field scattering and PL spectra methods were integrated into a microspectroscopy system based on an inverted optical microscope (NTEGRA Spectra, NT-MDT). As schematically depicted in Fig. 1a, the scattering spectra of the nanoparticles were measured using a white light total internal reflection scattering method based on a high numerical

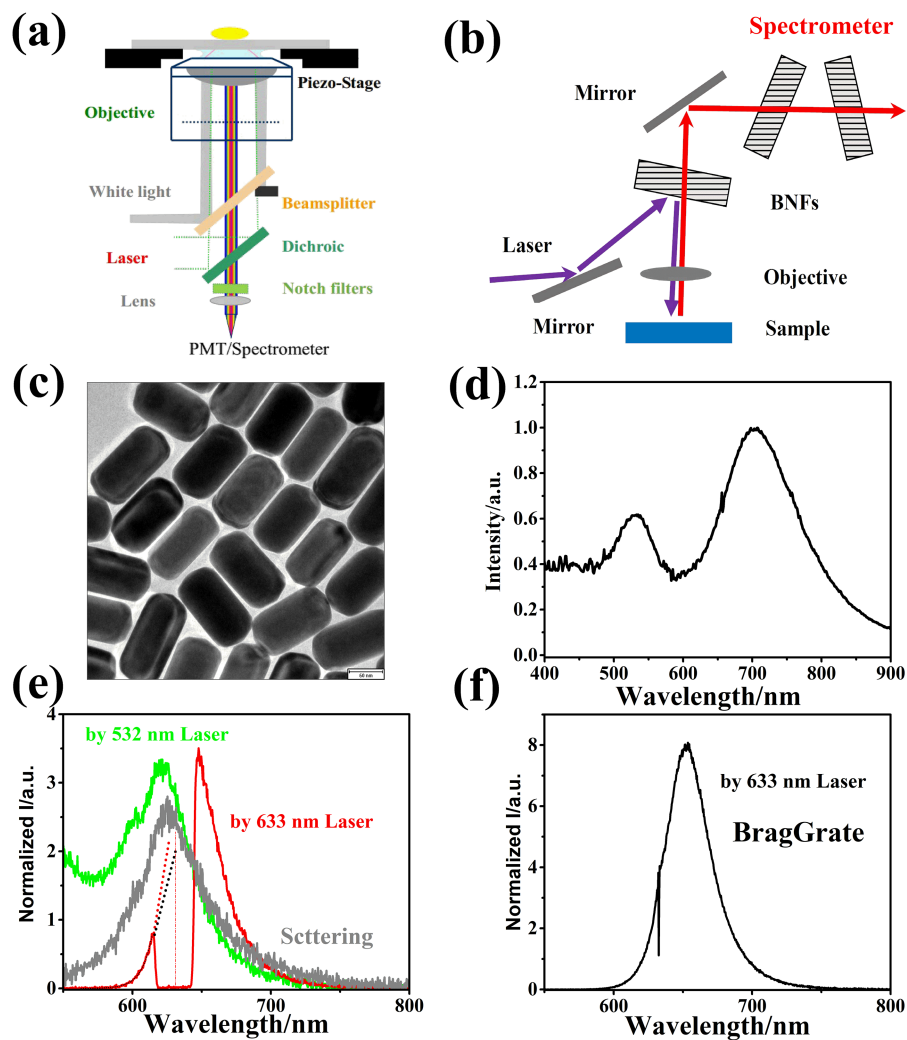


FIG. 1. (a) Schematic of experiment setup for single nanoparticle spectroscopy with interference notch filters. (b) Schematic diagram of single monochromator system with three VBG-based notch filters. (c) Representative SEM image of the synthesized gold nanorods (60-nm scale bar). (d) Extinction spectrum of the gold nanorods solution (e) PL spectra excited by 532- and 633-nm lasers with interference notch filters and corresponding scattering spectrum of the same gold nanorod, fitting curves of the anti-Stokes emission (black dots are for Fermi–Dirac distribution and red dots for Bose–Einstein distribution). (f) PL spectra of a single GNR excited by 633-nm laser with VBG-based notch filters.

aperture oil-immersion objective lens (N.A. 1.49, Olympus). Meanwhile, the microspectroscopy system could be easily switched from measuring the scattering spectrum to measuring PL. For PL observations, the samples were excited by a CW laser at  $\lambda = 532$  or  $633$  nm at room temperature with interference notch filters (Semrock Inc.). Single nanoparticles were selected by correlating scanning optical confocal imaging and atomic force microscopy imaging.<sup>13</sup> We corrected the PL spectrum of the GNR by subtracting the spectrum collected from a blank glass substrate near to the particle. To obtain the full-spectra line shape with an ultra-narrow notch band, VBG-based notch filters (OptiGrate Corp.) were applied in a Jobin-Yvon HR800 Raman system with laser excitation at  $633$  and  $676$  nm, as shown schematically in Fig. 1b.<sup>14</sup> This experimental configuration allowed for ultralow frequency Raman spectroscopy measurements; full details of this technique have been described elsewhere.<sup>14</sup> The gold nanorods were synthesized by a seed-mediated method. All chemicals were obtained from commercial sources and were used without further purification. The synthesis process has been described in detail in a previous report.<sup>13</sup> Representative SEM images and extinction spectrum of the synthesized GNRs are shown in Fig. 1 c and d, respectively. The gold nanorods were immobilized onto silane functionalized glass coverslips in a manner similar to our previous report for gold nanospheres with an average interparticle spacing of several micrometers.<sup>15</sup> Such an interparticle spacing is suitable for the identification of isolated nanorods by the microspectroscopy system because the diffraction-limited spots are sufficiently separated so as not to overlap.<sup>16</sup>

Previous reports on the emission spectra of gold nanoparticles have been collected mainly with the use of interference optical filters, which prevent extraction of the complete spectral shape near the excitation wavelength.<sup>4,10,11</sup> Fig. 1e shows representative PL and scattering spectra of the same individual GNR. The PL spectral shape, under excitation by the  $532$ -nm laser, closely resembles the scattering spectral shape for the GNR's longitudinal LSP mode. However, there is a considerable anti-Stokes emission component under excitation at  $633$  nm. As the excitation wavelength approaches plasmon resonance, the relative intensity of the anti-Stokes emission increased owing to plasmonic enhancement effects.<sup>10</sup> Huang *et al.* used a Bose–Einstein-like distribution function to fit the spectral line shape of the anti-Stokes emission,<sup>11</sup> while He *et al.* claimed that the line shape of anti-Stokes emission should follow a Fermi–Dirac distribution.<sup>10</sup> This controversy can be mainly attributed to incomplete measurements of the spectral shape. For example, as shown in Fig. 1e, interference notch filters block the emission over a wavelength ranging from  $617$  to  $645$  nm ( $\sim 87$  meV). The exponential trend of both fitting curves (black dots for Fermi–Dirac-like and red dots for Bose–Einstein-like line shape in Fig. 1e) appears to be reasonable in the range away from the excitation wavelength; however, the fitting lines deviate from each other near the excitation wavelength. In particular, the emission intensity was infinite at the excitation wavelength for the Bose–Einstein-like fitting. The use of VBG-based notch filters in the optical setup considerably improved the ability to obtain an almost complete spectral shape of the GNR light emission.<sup>14</sup> The ultra-narrow blocking bandwidth of the VBG-based notch filters enabled both Stokes and anti-Stokes emission to be observed simultaneously. The PL spectra of a GNR measured with VBG-based notch filters is shown in Fig. 1f for comparison. The VBG-based notch filters only blocked emission from  $632.6$  to  $632.9$  nm ( $\sim 1$  meV). The intensity of anti-Stokes emission increases exponentially as the excitation wavelength is approached, but remains at a finite value. This suggests that the PL emission intensity at the excitation wavelength should not be infinite as predicted by the Bose–Einstein distribution. Conversely, the Fermi–Dirac distribution fits the spectra well, based on the electron distribution near the Fermi level.

To elucidate the spectral line shape, two spectra of the GNR emission measured with two different VBG-based filters are shown in Fig. 2a, revealing the separation between the LSP band maximum and the excitation wavelength. The emission spectra were plotted as a function of photon energy, as shown in Fig. 2b to reveal their line shape. For Stokes emission, the spectral shape followed a Lorentzian line shape (red and green solid lines), which implies that the LSP mode determines the spectral shape of the Stokes emission. However, the emission in the anti-Stokes range could not be reproduced by the Lorentzian line shape; however, it could be well fitted by an exponential Fermi–Dirac-like distribution (blue solid lines in Fig. 2b). On the basis of these observations, it is reasonable to claim that the spectrum of the GNR emission obeys a Fermi–Dirac-like distribution rather than a Bose–Einstein-like distribution. As shown by Fig. 2c, the electron distribution near the Fermi level follows a thermal distribution, which is related to the anti-Stokes emission, whereas the electron

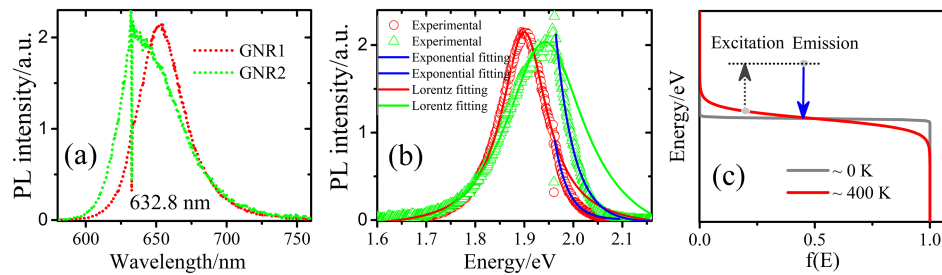


FIG. 2. (a) Representative PL spectra of two different GNRs measured with VBG-based notch filters. (b) PL spectra measured with the VBG-based filters shown in (a) plotted as function of photonic energy, solid lines (red and green) are fitted with Lorentzian line shape, while anti-Stokes emission (blue) is fitted by the Fermi–Dirac distribution. (c) Schematic of electron Fermi–Dirac distribution, excitation and transition process.

state density is constant under the Fermi level and related to the Stokes emission. Hence, the electron distribution and LSP mode jointly determines the spectral shape of the PL emission. Notably, multiple photon processes or electron excitation can also induce luminescence of the metal nanostructures, here we only focus on one-photon luminescence processes. Furthermore, ultra-narrow-band filters cannot be applied to extract the ultralow shift spectral information for two-photon luminescence of the plasmonic nanostructure owing to the spectral width of short pulse lasers.

In general, the light emission of the GNRs after photon excitation can be divided into two parts: elastic Rayleigh scattering of incident light and inelastic radiation (i.e., PL) based on the concept of a quantized plasmonic cavity.<sup>12</sup> Hence, the intensity of so-called PL emission of the plasmonic nanostructures at the excitation frequency is finite, and the PL quantum efficiency is several orders of magnitude lower than that of Rayleigh scattering.<sup>17</sup> Considering the energy band theory, light emission also depends on the electron distribution near the Fermi energy level, as shown in Fig. 2c. Anti-Stokes emission, i.e., at the high-energy side of the laser, owing to thermal smearing of the electron and hole distributions, can be described well by the Fermi–Dirac distribution function. Furthermore, the spontaneous radiative transition rate obeys Fermi’s golden rule such that the transition rate is determined by the electron and photonic density of states. Hence, the PL spectral line shape of the GNR excited by a CW laser is governed by the LSP mode and the electron distribution.<sup>12</sup>

Usually, intraband transitions dominate the light emission processes when gold nanostructures are excited by a 785-nm CW laser ( $\sim 1.58$  eV).<sup>4</sup> This effect arises because the energy separation between *d-band* holes and the Fermi surface of gold is approximately 1.8 eV near the X point, and 2.4 eV near the L point, interband transitions is not possible. We also observed the PL of the gold nanostructures at different excitation wavelengths of 676 nm (1.83 eV), 633 nm (1.96 eV), and 532 nm (2.33 eV). Representative results are summarized in Fig. 3. To match with the 532-nm laser, gold nanoparticles (nominal spherical shape) with an LSP resonance at  $\sim 550$  nm were also investigated. A clear and strong anti-Stokes emission band was present for all the different nanoparticles. This clear anti-Stokes emission band remained at different excitation wavelengths and even for excitation close to the interband transition. On the basis of the plasmon emission mechanism, hot electrons in a conductive band could recombine non-radiatively to emit LSP plasmons. These plasmons subsequently radiate, giving rise to the observed PL, and the plasmon radiation rate was modified by the photonic states density.<sup>6,18</sup> However, for the electron states, the electron Fermi–Dirac distribution influences the spectral shape. For anti-Stokes emission, the electron distribution near the Fermi level is defined by an exponential function. Thus, the line shape of the anti-Stokes emission has an exponential-like line shape.

Following rules of the Fermi–Dirac distribution,  $f(E) = 1/(Ae^{E/KT} + 1)$ , the electron distribution depends on the electron temperature. Thus, the temperature should have a strong influence on the PL spectral properties. For example, anti-Stokes intensity was shown to increase as temperature was increased in the pioneer work by Mooradian.<sup>1</sup> In that report, the anti-Stokes emission intensity was greater at a high temperature of 300 K than that at 10 K for bulk gold materials.<sup>1</sup> Recently, Hugall *et al.* also reported the temperature dependence of anti-Stokes emission of gold periodic inverted pyramid in detail.<sup>19</sup> Here, the excitation power dependent spectra of the GNR were investigated.

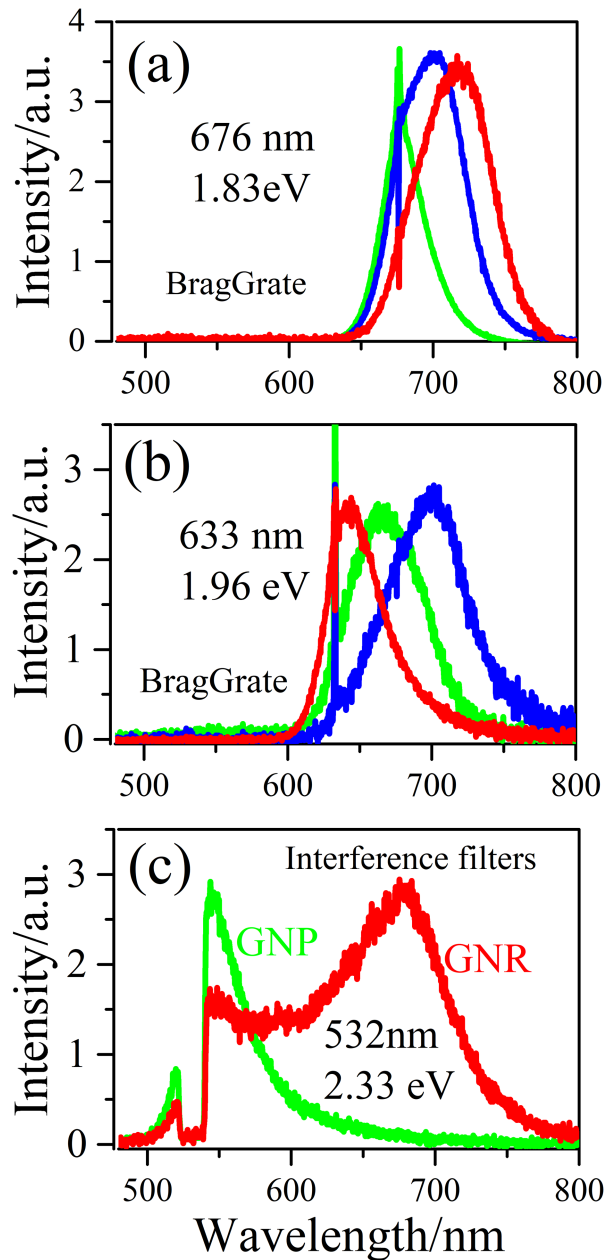


FIG. 3. PL spectra with excitation by CW lasers at: (a) 676 nm and (b) 633 nm with VBG-based notch filters for six different GNRs with different detuning frequencies according to the excitation source, and (c) excitation by a 532-nm laser with the use of interference filters.

The intensity of the anti-Stokes and Stokes emission both increased almost linearly as the power was increased. However, the intensity of the anti-Stokes emission increased faster than that of the Stokes emission, indicated clearly by their ratio as a function of the excitation power, as shown in Fig. 4c. Owing to photothermal effects, the temperature of the GNR increased as the excitation power was increased. This effect was particularly noticeable when the LSP band matched well with the excitation wavelength, as shown Fig. 4, i.e. on resonant excitation. We noted that the ratio remained constant or changed slightly if the LSP band was far from the excitation wavelength, because the absorption cross-section is larger for resonant excitation resulting in higher local temperature of the GNRs.<sup>20</sup> These results imply that the Fermi–Dirac distribution of the electrons in the *sp* band is the main factor influencing the spectral shape of light emission from plasmonic nanostructures.<sup>10,21</sup>

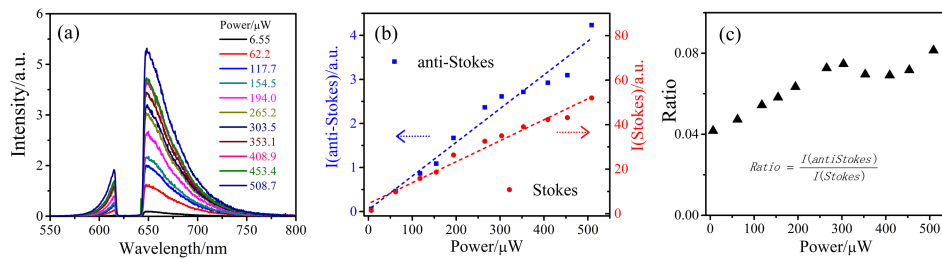


FIG. 4. Excitation power dependent PL spectra of a GNR. (a) PL spectra of a GNR measured under different excitation powers. (b) Integrated intensity of Stokes and anti-Stokes emission as a function of excitation power; the dash lines show linear fitting curves. (c) Ratio of anti-Stokes to Stokes emission intensity as a function of excitation power.

In summary, light emission spectra of single gold nanorods was measured with the use of notch filters with ultra-narrow bandwidths. We confirmed that the Stokes emission spectral shape dominated by LSP resonance could be fitted by a Lorentzian line shape. In contrast, the anti-Stokes emission spectral shape could be fitted well with a Fermi–Dirac-like line shape, indicating that this emission is governed by the electron distribution near the Fermi level. The anti-Stokes emission band could be observed under different excitation wavelengths. The electron distribution could influence the spectral shape of anti-Stokes emission for both interband and intraband transitions. We also found that anti-Stokes emission intensity increased more rapidly as the temperature increased. These findings contribute to a deeper understanding of light emission from plasmonic nanostructures.

## ACKNOWLEDGMENTS

This work was supported by the National Key Basic Research Program of China (grant no. 2013CB328703), the National Key Research and Development Program of China (grant nos. 2016YFA0301204 and 2017YFA0303700), the National Natural Science Foundation of China (grant nos. 61422502, 11374026, 61521004, 11527901, 11434010 and 11474277).

- <sup>1</sup> A. Mooradian, *Phys. Rev. Lett.* **22**, 185 (1969).
- <sup>2</sup> G. T. Boyd, Z. H. Yu, and Y. R. Shen, *Phys. Rev. B* **33**, 7923 (1986).
- <sup>3</sup> M. B. Mohamed, V. Volkov, S. Link, and M. A. El-Sayed, *Chem. Phys. Lett.* **317**, 517 (2000).
- <sup>4</sup> M. R. Beversluis, A. Bouhelier, and L. Novotny, *Phys. Rev. B* **68**, 115433 (2003).
- <sup>5</sup> J. Mertens, M. E. Kleemann, R. Chikkaraddy, P. Narang, and J. J. Baumberg, *Nano Lett.* **17**, 2568 (2017).
- <sup>6</sup> E. Dulkeith, T. Niedereichholz, T. Klar, J. Feldmann, G. von Plessen, D. Gittins, K. Mayya, and F. Caruso, *Phys. Rev. B* **70**, 205424 (2004).
- <sup>7</sup> M. Yorulmaz, S. Khatua, P. Zijlstra, A. Gaiduk, and M. Orrit, *Nano Lett.* **12**, 4385 (2012).
- <sup>8</sup> D. Sivun, C. Vidal, B. Munkhbat, N. Arnold, T. A. Klar, and C. Hrelescu, *Nano Lett.* **16**, 7203 (2016).
- <sup>9</sup> B. Neupane, L. Y. Zhao, and G. F. Wang, *Nano Lett.* **13**, 4087 (2013).
- <sup>10</sup> Y. He, K. Xia, G. Lu, H. Shen, Y. Cheng, Y. C. Liu, K. Shi, Y. F. Xiao, and Q. Gong, *Nanoscale* **7**, 577 (2015).
- <sup>11</sup> J. Huang, W. Wang, C. J. Murphy, and D. G. Cahill, *PNAS* **111**, 906 (2014).
- <sup>12</sup> K. Xia, Y. He, H. Shen, Y. Cheng, Q. Gong, and G. Lu, *Proc. SPIE* **9668**, 96685B (2015).
- <sup>13</sup> T. Zhang, H. Shen, G. Lu, J. Liu, Y. He, Y. Wang, and Q. Gong, *Adv. Opt. Mater.* **1**, 335 (2013).
- <sup>14</sup> P. H. Tan, W. P. Han, W. J. Zhao, Z. H. Wu, K. Chang, H. Wang, Y. F. Wang, N. Bonini, N. Marzari, N. Pugno, G. Savini, A. Lombardo, and A. C. Ferrari, *Nat. Mater.* **11**, 294 (2012).
- <sup>15</sup> Q. Wang, G. Lu, L. Hou, T. Zhang, C. Luo, H. Yang, G. Barbillon, F. H. Lei, C. A. Marquette, P. Perriat, O. Tillement, S. Roux, Q. Ouyang, and Q. Gong, *Chem. Phys. Lett.* **503**, 256 (2011).
- <sup>16</sup> G. Lu, Y. Wang, R. Y. Chou, H. Shen, Y. He, Y. Cheng, and Q. Gong, *Laser Photon. Rev.* **9**, 530 (2015).
- <sup>17</sup> Y. Cheng, G. Lu, Y. He, H. Shen, J. Zhao, K. Xia, and Q. Gong, *Nanoscale* **8**, 2188 (2016).
- <sup>18</sup> A. Tcherniak, S. Dominguez-Medina, W.-S. Chang, P. Swanglap, L. S. Slaughter, C. F. Landes, and S. Link, *J. Phys. Chem. C* **115**, 15938 (2011).
- <sup>19</sup> J. T. Hugall and J. J. Baumberg, *Nano Lett.* **15**, 2600 (2015).
- <sup>20</sup> S.-W. Chu, H.-Y. Wu, Y.-T. Huang, T.-Y. Su, H. Lee, Y. Yonemaru, M. Yamanaka, R. Oketani, S. Kawata, S. Shoji, and K. Fujita, *ACS Photonics* **1**, 32 (2014).
- <sup>21</sup> A. Carattino, V. I. P. Keizer, M. J. M. Schaaf, and M. Orrit, *Biophys. J.* **111**, 2492 (2016).